



# Interaction mechanisms between slurry coatings and solid oxide fuel cell interconnect alloys during high temperature oxidation

Å.H. Persson<sup>a,\*</sup>, L. Mikkelsen<sup>a,1</sup>, P.V. Hendriksen<sup>a,2</sup>, M.A.J. Somers<sup>b</sup>

<sup>a</sup> Division of Fuel Cells and Solid State Chemistry, Risø National Laboratory for Sustainable Energy, Technical University of Denmark, P.O. 49, DK-4000 Roskilde, Denmark

<sup>b</sup> Department of Mechanical Engineering, Technical University of Denmark, Kemitorvet b.204, DK-2800 Lyngby, Denmark

## ARTICLE INFO

### Article history:

Received 28 October 2011

Received in revised form

16 December 2011

Accepted 19 December 2011

Available online 20 January 2012

### Keywords:

Oxidation

Microstructure

Diffusion

Surfaces and interfaces

Fuel cells

Coating materials

## ABSTRACT

Six different coatings consisting of fluorite-, corundum-, spinel- or perovskite-type oxides were deposited on a Fe22Cr alloy (Crofer 22APU) and oxidized at 900 °C in moisturized air.

Five of the coatings prevented break-away oxidation otherwise observed for the uncoated alloy, and the parabolic oxidation rate constant was reduced with 50–90% of that for uncoated alloy. One coating consisting of MnCo<sub>2</sub>O<sub>4</sub> did not significantly affect the oxidation rate of the alloy, and just as for uncoated samples break-away oxidation occurred for MnCo<sub>2</sub>O<sub>4</sub> coated samples. The interaction mechanisms between the growing oxide scales and applied coatings can be classified according to three types.

© 2012 Elsevier B.V. All rights reserved.

## 1. Introduction

In a solid oxide fuel cell (SOFC)-stack the interconnect is the component in-between the cathode of one fuel cell and the anode of the next fuel cell. The interconnect also separates the air from the fuel in adjoining cells of a stack. The interconnect material has to be chemically and thermally compatible with the other cell components from room temperature up to operational temperature of the fuel cells, approximately 750–850 °C [1]. Ferrous Cr<sub>2</sub>O<sub>3</sub> (chromia) forming alloys have shown promising results as interconnect materials. They are cheap, easy to shape and handle and they meet many of the requirements on interconnect plates including high electrical conductivity, gas tightness, and matching thermal expansion with the cell. Chromia-forming alloys present a good balance between a slow growth rate of the oxide scale and electrical conductivity of the oxide scale in comparison to alumina and silica forming alloys, which have a significantly higher electrical resistance in the forming oxide scale [1–4]. However, for the SOFC-stack

to present satisfying operational efficiency the growth rates and the electrical resistance of the oxide scale have to be decreased even further. It would further be beneficial if the chromium content in the protecting oxide scale would be decreased, since chromium species evaporating or diffusing via surfaces from the chromia scale, have a detrimental poisonous effect on the fuel cell. The chromium species tend to diffuse into the cathode/electrolyte interface, where the chromium species block the catalytic reactive sites [1,2,5–7]. Alloys forming a duplex scale consisting of an inner Cr<sub>2</sub>O<sub>3</sub> phase and an outer MnCr<sub>2</sub>O<sub>4</sub> phase have been developed in the last years and have shown promising results in decreasing chromium evaporation [2,5,8,9]. However, the oxidation rate, the electrical resistivity and the amount of the chromium in the outmost of the oxide scale on the interconnect alloys has still not been decreased enough for use in a commercial SOFC-stacks [1,5,9,10]. Application of coatings to improve the suitability of Crofer, and other chromia-forming alloys, has previously been demonstrated to be a promising route for further advancement [8,11–16]. Utilizing coatings has shown to decrease the oxidation rate of the alloys, and to decrease the electrical resistance of the formed oxides as well as to reduce the chromium evaporation and diffusion from the oxide surface [11,17–20]. To get a more detailed understanding of how coatings and steel interact, oxidation experiments of slurry coated Crofer 22APU were carried out. Coatings consisting of oxides belonging to different structure classes, fluorite, corundum, spinel and perovskite, and with very different chemical properties

\* Corresponding author. Tel.: +45 21 32 54 93; fax: +45 4677 5858.

E-mail addresses: [aase@risoe.dtu.dk](mailto:aase@risoe.dtu.dk) (Å.H. Persson), [larm@risoe.dtu.dk](mailto:larm@risoe.dtu.dk) (L. Mikkelsen), [pvhe@risoe.dtu.dk](mailto:pvhe@risoe.dtu.dk) (P.V. Hendriksen), [somers@mek.dtu.dk](mailto:somers@mek.dtu.dk) (M.A.J. Somers).

<sup>1</sup> Tel.: +45 4677 5811.

<sup>2</sup> Tel.: +45 4677 5725.

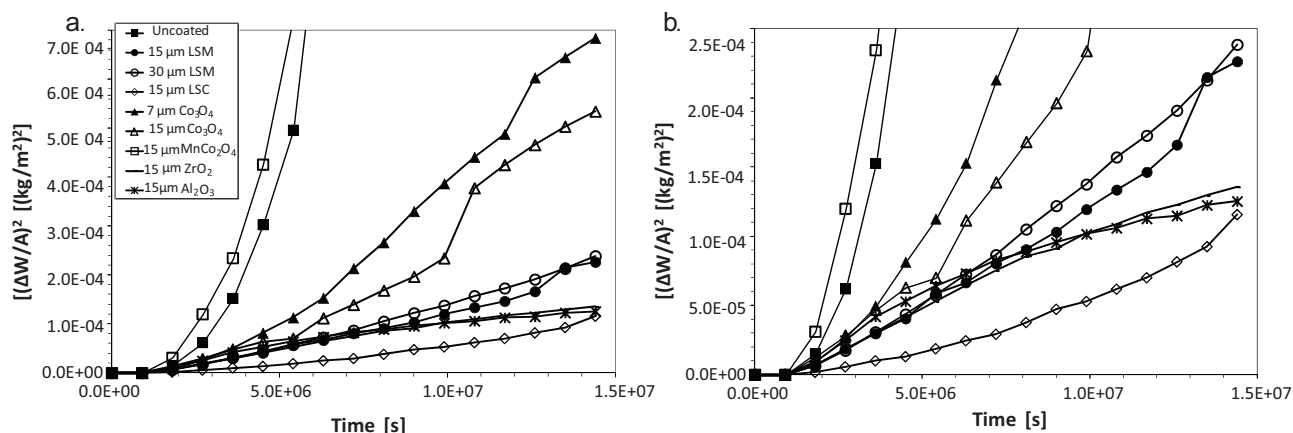


**Fig. 1.** The  $(\Delta W/A)^2$ –time plots for uncoated and coated Crofer 22APU samples in the long-term, cyclic oxidation experiment carried out at 900 °C in air containing 1% water vapour, (a) overview, (b) enlargement of (a) for relatively small weight increase, the key is the same for both plots.

were applied. The coatings included in the study were  $\text{Al}_2\text{O}_3$ ,  $\text{ZrO}_2$ ,  $(\text{La}_{0.85}\text{Sr}_{0.15})_{1-x}\text{Mn}_{1+x}\text{O}_3 + (0.1-x)\text{Mn}_2\text{O}_3$  (referred to as LSM),  $\text{MnCo}_2\text{O}_4$ , 90 wt.%  $(\text{La}_{0.85}\text{Sr}_{0.15})\text{CoO}_3 + 10$  wt.%  $\text{Co}_3\text{O}_4$  (referred to as LSC), and  $\text{Co}_3\text{O}_4$ . None of the applied coatings contain Cr as one of the roles of the coating is to reduce the Cr activity on the surface of the coated steel to reduce the Cr evaporation rate. The chemical stability of the coating materials varies strongly over the series of materials (listed above in order of reducing stability). Whereas  $\text{Al}_2\text{O}_3$  and  $\text{ZrO}_2$  are extremely stable compounds (reduction  $p\text{O}_2$  at 900 °C for  $\text{Al}_2\text{O}_3 = 1.4 \times 10^{-39}$  atm and  $\text{ZrO}_2 = 9.6 \times 10^{-40}$  atm [21]) the most unstable compounds used  $\text{Co}_3\text{O}_4$  and LSC would decompose already during heating in air or under mild reduction (e.g. reduction  $p\text{O}_2$  at 900 °C for  $\text{CoO} = 3.2 \times 10^{-14}$  atm [21]), and hence very different interaction mechanisms between coating and steel could be anticipated over this series of materials. It should be noted that a technologically viable SOFC interconnect coating must provide good conductivity in the interface between interconnect and electrode. Whereas the four latter materials are good electronic conductors (e.g.  $\sigma_{\text{LSC}} > 1000$  S/cm in air at 900 °C [22]) the two former ( $\text{Al}_2\text{O}_3$  and  $\text{ZrO}_2$ ) are poor electronic conductors (e.g.  $\sigma_{\text{Al}_2\text{O}_3} < 10^{-7.5}$  S/cm in air at 1200 °C [23]). These materials are thus not directly applicable as single phase coatings in SOFC-stacks. The results allowed classifications of interaction mechanisms that can pave the road towards optimal coating designs.

## 2. Experimental

Crofer 22APU samples with the dimension 20 mm  $\times$  20 mm  $\times$  0.3 mm were etched for 30 min in a mixture of 75 vol.%  $\text{H}_2\text{O}$  + 5 vol.%  $\text{HF}$  + 20 vol.%  $\text{HNO}_3$ , to remove any native oxides formed during alloy processing. A series of samples was slurry coated on both sides using a hand held spray-gun, so that oxide thicknesses of approximately 7, 15 or 30  $\mu\text{m}$  were applied. Simultaneously as the corrosion samples were sprayed a reference sample was sprayed, and the thickness of the applied coating on this reference sample was measured with a caliper. The coatings included in this study were  $\text{ZrO}_2$ ,  $\text{Al}_2\text{O}_3$ ,  $\text{Co}_3\text{O}_4$ ,  $\text{MnCo}_2\text{O}_4$ , LSM, and LSC. The slurries consisted of approximately 33 wt.% powder of the coating material dissolved in ethanol with a small amount of polyvinyl pyrrolidone, (PVP)-binder. Before spraying onto the alloy substrates, the LSM, LSC,  $\text{Co}_3\text{O}_4$  and  $\text{MnCo}_2\text{O}_4$  slurries were ball-milled until a particle size of  $\phi_{\text{median}} = 1\text{--}2$   $\mu\text{m}$  was achieved and the  $\text{ZrO}_2$ ,  $\text{Al}_2\text{O}_3$  slurry was ball-milled until a particle size of approximately  $\phi_{\text{median}} = 3$   $\mu\text{m}$  was achieved.

The etched uncoated samples and the coated samples were weighed before mounting in the oxidation furnace with a volume of approximately  $4.32 \times 10^{-3}$   $\text{m}^3$ . Air containing 1% water vapour was lead through the furnace with a flow rate of approximately  $72 \times 10^{-3}$   $\text{m}^3/\text{h}$ . The samples were oxidized in 250-h cycles at 900 °C, after which they were weighed. The heating and cooling ramps were set to 120 °C/h. The total accumulated oxidation time was 4000 h. With a few exceptions, six samples of each corrosion sample type were prepared, corroded and removed from the furnace for further investigation after 500, 1000, 2000, and 4000 h of oxidation.

On one of the epoxy mounted  $\text{Al}_2\text{O}_3$  coated samples, Focused Ion Beam (FIB) was used to prepare a Transmission Electron Microscope (TEM) sample for more

detailed analysis of the alloy/oxide and oxide/coating interfaces and the oxide scale itself.

## 3. Results

### 3.1. Weight gain and microstructure

The weight gain data collected for the uncoated and coated Crofer samples during the cyclic oxidation experiment are presented as a weight increase<sup>2</sup>–time plot in Fig. 1.

The plots of the uncoated Crofer sample and the Crofer samples coated with LSM, LSC,  $\text{Co}_3\text{O}_4$ , and  $\text{MnCo}_2\text{O}_4$  are linear in Fig. 1 up to 1000 h oxidation, where break-away oxidation takes place for the uncoated and  $\text{MnCo}_2\text{O}_4$  coated samples. The weight gain of the uncoated and  $\text{MnCo}_2\text{O}_4$  coated samples was immense and since break-away oxidation was detected at an early stage the weight gain of these samples were ignored when zooming in on the weight gain of the rest of the samples in the study. Note, that the LSM, LSC, and  $\text{Co}_3\text{O}_4$  coated samples continue to present linear behaviour up to 4000 h oxidation. The linearity in the weight increase<sup>2</sup>–time plot indicates parabolic oxidation kinetics, as described by the expression in Eq. (1):

$$\Delta w^2 = k_p t_t + C, \quad (1)$$

$\Delta w$  is the weight gain, while  $k_p$  and  $t_t$  are the parabolic rate constant and oxidation time, respectively.  $C$  is an integration constant correcting for transient oxidation, and here also for binder burn off from the coatings, which governs the initial weight measurements. Accordingly the first 250 h of oxidation is neglected. Parabolic oxidation indicates that the oxidation rate is determined by a diffusion process with constant diffusion coefficient resulting in a growth rate that decreases inversely proportionally to the oxide layer thickness [24].

The weight increase<sup>2</sup>–time curves of the  $\text{Al}_2\text{O}_3$  and  $\text{ZrO}_2$  coated Crofer samples in Fig. 1 suggest deviations from parabolic oxidation, reflecting alternative reaction mechanisms in the system, i.e. the protective action of the scale effectively increases over time. The weight gain curves of the  $\text{Al}_2\text{O}_3$  and  $\text{ZrO}_2$  coated samples are deflected downwards, while the weight gain curves of all the other samples in this study are either linear or deflecting ever so slightly upwards.

Apart from  $\text{MnCo}_2\text{O}_4$  all the coatings lowered the weight gain compared to the uncoated Crofer 22APU. The parabolic oxidation constants for the uncoated and the coated Crofer 22APU samples are summarized in Tables 1a and 1b. For the  $\text{Co}_3\text{O}_4$  coated sample a slight increase in the parabolic oxidation constant was observed

Download English Version:

<https://daneshyari.com/en/article/1616251>

Download Persian Version:

<https://daneshyari.com/article/1616251>

[Daneshyari.com](https://daneshyari.com)